PERGAMON

Vision Research 39 (1999) 3465–3479

Vision Research

www.elsevier.com/locate/visres

Section 4

MT neurons in the macaque exhibited two types of bimodal direction tuning as predicted by a model for visual motion detection

Hiroaki Okamoto [a,*], Susumu Kawakami [a], Hide-aki Saito [b], Eiki Hida [b], Keiichi Odajima [b], Daichi Tamanoi [b], Hiroshi Ohno [b]

[a] *Fujitsu Laboratories Ltd, 4-1-1 Kamikodanaka, Nakahara-ku, Kawasaki 211-8588, Japan*
[b] *Tamagawa University, Faculty of Engineering, 6-1-1 Tamagawagakuen, Machida, Tokyo 194-8610, Japan*

Received 28 July 1998; received in revised form 25 January 1999

Abstract

We previously proposed a model for detecting local image velocity on the magnocellular visual pathway (Kawakami & Okamoto (1996) *Vision Research*, *36*, 117–147). The model detects visual motion in two stages using the hierarchical network that includes component and pattern cells in area MT. To validate the model, we predicted two types of bimodal direction tuning for MT neurons. The first type is characteristic of component cells. The tuning is bimodal when stimulated with high-speed spots, but unimodal for low-speed spots or for bars. The interval between the two peaks widens as the spot's speed increases. The second type is characteristic of pattern cells. The tuning is bimodal when stimulated with low-speed bars, but unimodal for high-speed bars or for spots. The interval widens as the bar's speed decreases. To confirm this prediction, we studied the change of direction tuning curves for moving spots and bars in area MT of macaque monkeys. Out of 35 neurons measured at various speeds, six component cells and four pattern cells revealed the predicted bimodal tunings. This result provided neurophysiological support for the validity of the model. We believe ours is the first systematic study that records the two types of bimodality in MT neurons.

Keywords: Network model; Local image velocity; Bimodal direction tuning; Single cell response; Area MT

1. Introduction

The middle temporal area (MT) in the visual cortex is known as the center of local motion detection. Each neuron in area MT selectively responds to a particular direction of visual stimuli within a small region on the retina but does not respond to a movement in the opposite direction (Zeki, 1974; Maunsell & Van Essen, 1983; Albright, 1984; Maunsell & Newsome, 1987). The neurons are also sensitive to the speed of visual motion (Maunsell & Van Essen, 1983; Albright, 1984; Mikami, Newsome & Wurtz, 1986a,b; Maunsell & Newsome, 1987; Lagae, Raiguel & Orban, 1993). Thus, MT neurons are considered capable of analyzing the velocity (i.e. direction and speed) of visual stimuli.

Movshon, Adelson, Gizzi and Newsome (1985) found that the MT neurons of monkeys can be classified into two distinct types according to sensitivity to plaid patterns, i.e. the sum of two differently oriented moving gratings. One class, referred to as component-motion selective cells (component cells), responds best to a moving plaid pattern when the axis of motion of one of the component gratings coincides with the cell's preferred axis of motion. In contrast, the other class, called pattern-motion selective cells (pattern cells), responds best when the axis of motion of the plaid pattern itself coincides with the cell's preferred axis of motion. That is, component cells analyze the motion of each component grating whereas pattern cells analyze the motion of the plaid pattern as a whole. It was also reported that component cells account for about 40% of MT neurons and exist mainly in layers 4, 6 of MT. On the other hand, pattern cells account for

* Corresponding author. Fax: +81-447542693.
E-mail address: okamoto@flab.fujitsu.co.jp (H. Okamoto)

0042-6989/99/$ - see front matter
PII: S0042-6989(99)00073-5

about 25% of MT neurons and exist mainly in layers 2, 3, and 5 (Movshon et al., 1985).

On the basis of a variety of neurophysiological and psychophysical findings, many models for motion detection have been proposed. These models can be classified based on their approach; spatio-temporal correlation (Reichardt, 1961; Van Santen & Sperling, 1985; Borst & Egelhaaf, 1989), spatial and temporal luminance gradients (Fennema & Thompson, 1979; Marr & Ullman, 1981), and spatio-temporal filtering on the frequency domain (Adelson & Bergen, 1985; Watson & Ahumada, 1985; Heeger, 1987; Grzywacz & Yuille, 1990; Ogata & Sato, 1991; Sereno, 1993). Many of these models are based on the two-stage hypothesis proposed by Adelson and Movshon (1982) for motion perception in humans. In the first stage of the hypothesis, one-dimensional (1-D) velocities perpendicular to oriented components within a moving stimulus are analyzed. In the second stage, these velocities are recombined to detect the two-dimensional (2-D) velocity of the stimulus. Adelson and Movshon also proposed the intersection-of-constraint lines (IOC) solution for the recombination rule processed in the second stage.

In a previous paper (Kawakami & Okamoto, 1996), we proposed a model for detecting the local image velocity, which is based on a spatio-temporal correlation. The model described the whole network on the magnocellular visual pathway with a series of simple formulas possibly applicable to neurophysiology. The directionally selective complex (DS complex) cells in the model detect the 1-D velocities of moving stimuli, and, by integrating these 1-D velocities, the model's motion-detection cells finally detect the 2-D velocity. We suggested that the model DS complex and the model motion-detection cells were component and pattern cells, respectively.

This network model predicts that two types of bimodal direction tuning will be observed for the two types of MT neurons under specific conditions of the visual stimuli. The first type is characteristic of DS complex cells (i.e. component cells). The tuning is bimodal when stimulated with high-speed spots, but unimodal for low-speed spots or for bars of all speeds. The interval between the two peaks widens as the spot speed increases. The second type is characteristic of motion-detection cells (i.e. pattern cells). The tuning is bimodal when stimulated with low-speed bars, but unimodal for high-speed bars or for spots of all speeds. The interval widens as the bar speed decreases. In this way, each type of MT neurons reveals the distinct response properties for each kind of moving stimulus: a spot and a bar.

To confirm this prediction, we conducted an electrophysiological experiment in area MT of anesthetized and paralyzed monkeys. We first classified the isolated neuron as a component or pattern cell type based on its response to a moving cross. We then measured its direction tunings for moving spots and bars, changing speeds systematically. We recorded six component and four pattern cells showing bimodal direction tunings as predicted by the model. This supports the validity of the model neurophysiologically. We believe ours is the first report predicting bimodal tunings for moving spots and bars and observing these two types of bimodalities in area MT of macaque monkeys.

2. Theory

In this section, we outline our motion detection model and predict the bimodal direction tunings under specific conditions of visual stimuli. This model was presented in a previous paper (Kawakami & Okamoto, 1996).

2.1. Motion detection model

We modeled a network for motion detection by inserting a lagged branch into the magnocellular visual pathway. This network is composed of the five types of cells shown in Fig. 1: lateral geniculate nucleus (LGN) cells; nondirectionally selective (NDS) simple cells; directionally selective (DS) simple cells; DS complex cells; and motion-detection cells. Two classes of cells exist in the LGN: lagged cells; and nonlagged cells (Mastronarde, 1987a,b; Humphrey & Weller, 1988; Saul & Humphrey, 1990). Through branches of the lagged and nonlagged LGN cells, a moving object on the retina is divided into the lagged and nonlagged images. The local motion of the object can be detected as the spatial distance between these two images. We also propose the existence of a functional hierarchy constituted by these five cell types, as shown on the left in Fig. 1. Through a sequential processing (the Hough transform

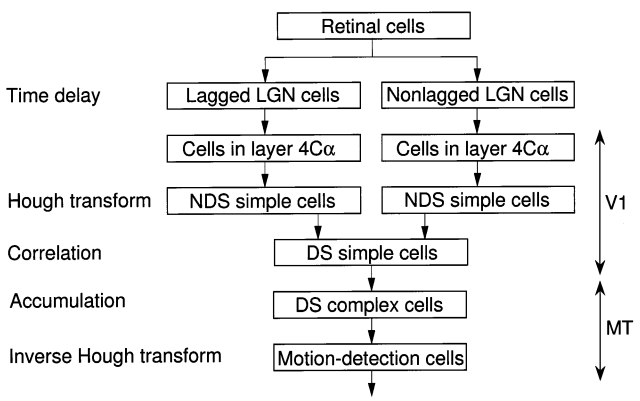

Fig. 1. Proposed visual pathway for detecting local image velocity. Five types of cells on this pathway constitute the functional hierarchy shown on the left. DS, directionally selective; NDS, nondirectionally selective.

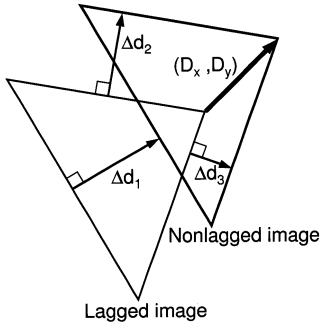

Fig. 2. Principal idea for motion detection in the model. A triangle is moving in an upward right direction. The spatial displacement between the lagged and nonlagged images is given by (D_x, D_y). Three component lines constructing the triangle move by Δd_i $(i = 1, 2, 3)$ in a direction perpendicular to the line, respectively. Integrating these displacements (Δd_i), the displacement vector (D_x, D_y) can be determined.

[Hough, 1962; Duda & Hart, 1972], a spatio-temporal correlation, and the inverse Hough transform) for the lagged and nonlagged images, local motion is finally detected in area MT.

The principal idea for velocity detection employed in the model is illustrated in Fig. 2. Consider a triangle moving in an upper right direction during a fixed time delay. The triangle is spatially displaced, and the displacement vector between the lagged and nonlagged images is represented by (D_x, D_y). The vector indicates the movement of the triangle as a whole, i.e. the 2-D velocity of the triangle. On the other hand, the displacement of each component line in a direction perpendicular to it, Δd_i $(i = 1, 2, 3)$, corresponds to the 1-D velocity of the line. Integrating the 1-D velocities of each component line, the 2-D velocity of the triangle can be determined. The relationship between the 1-D and 2-D velocities (Fig. 3) is represented by the following formulas.

$$V_{1D} = V_{2D}\boldsymbol{u} = V_{2D}\cos(\phi - \theta) = V_x \cos\theta + V_y \sin\theta \quad (1)$$

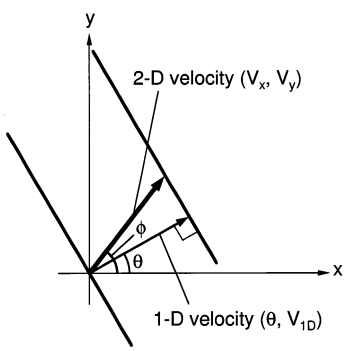

Fig. 3. Relationship between the 1-D and the 2-D velocities. The 1-D velocity of a line (V_{1D} speed and θ direction) is the orthogonal projection of its 2-D velocity (V_{2D} speed and ϕ direction) in a perpendicular direction. The 2-D velocity is also represented as (V_x, V_y) by Cartesian coordinates.

where

$$V_{2D} = (V_x, V_y) = V_{2D}\,(\cos\phi, \sin\phi)$$

and

$$\boldsymbol{u} = (\cos\theta, \sin\theta).$$

V_{1D}, θ, and $\boldsymbol{u}$ are the speed, direction and unit vector of the 1-D velocity, respectively. V_{2D}, ϕ, V_x, and V_y are the speed, direction, and Cartesian coordinates of the 2-D velocity, respectively.

The whole network of the model is illustrated in Fig. 4 on the basis of cell responses to a moving cross stimulus. This simple network accounted for a variety of physiological data on visual motion and detected the velocity of various kinds of visual stimuli such as single dots, lines, curves, random dots, natural scenes, and transparent movements (Kawakami & Okamoto, 1996).

2.2. Two types of directionally selective cells

Our model includes two types of directionally selective cells that perform the two-stage hypothesis. The DS complex cells detect the 1-D velocity in the first stage, and the motion-detection cells detect the 2-D velocity in the second stage. Actual MT neurons are also divided into two classes based on their directional selectivity. Movshon et al. (1985) studied the direction tuning of MT neurons using sinusoidal gratings and plaid patterns. A cell, sensitive only to the motion of the oriented components of the plaid, selectively responded only when the pattern stimulus contained one component moving in the preferred direction. This type of cell was called a component cell. In contrast, a cell truly sensitive to the motion of a pattern independent of its oriented components responded maximally when the direction of motion of the whole plaid matched the cell's preferred direction. This type of cell was called a pattern cell. Succinctly, component cells are sensitive to the 1-D velocity, and pattern cells are sensitive to the 2-D velocity.

Comparing the properties of the modeled cells with those of actual MT neurons, we believe that the modeled DS complex and motion-detection cells are component and pattern cells. The laminar distribution of component (mainly in layers 4, 6) and pattern cells (mainly in layers 2, 3, 5) reported by Movshon et al. (1985) also provides evidence of a hierarchy of two types of MT neurons.

2.3. Bimodal direction tunings

The model predicts that two types of bimodal direction-tuning curves will be observed for two types of model MT cells, DS complex cells and motion-detection cells, respectively.

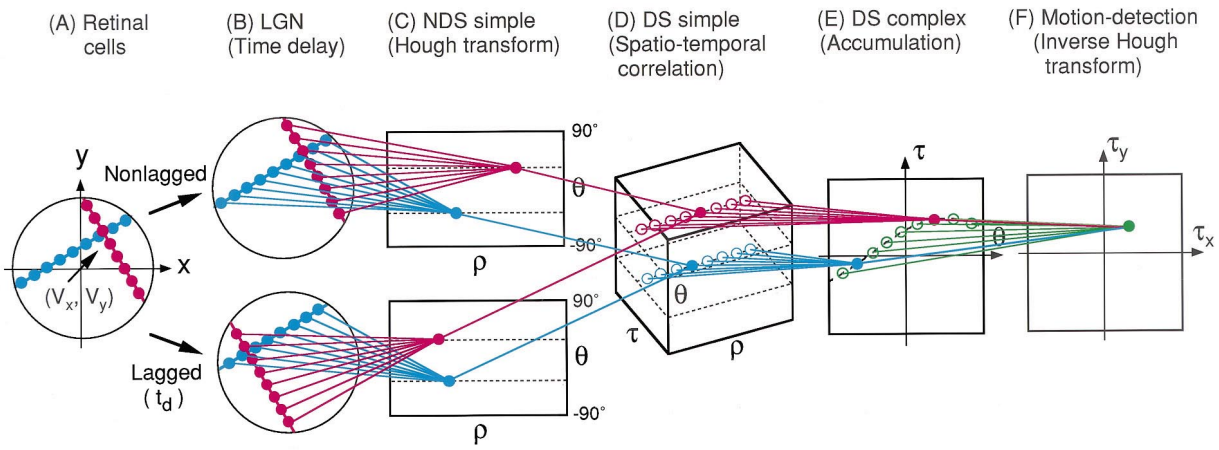

Fig. 4. Schematic representation of the modeled network for detecting the 2-D velocity of a moving cross. Circles indicate cells, and filled circles indicate the intensively activated cells on each cell array. Only connections between the activated cells are depicted; other cells and connections are not depicted. (A) Retinal image of the moving cross. (B) The lagged and nonlagged images on the LGN cells. (C) Hough transformation of lines of the cross. Each line is transformed into a corresponding point. (D) Two NDS simple cells are activated to detect the coincidence between lagged and nonlagged NDS simple cell responses. (E) Accumulating the DS simple cell responses along ρ coordinates, two DS complex cells are activated. The cells are located on a sine wave that corresponds to the 2-D velocity. (F) Through the inverse Hough transformation of the DS complex cell responses on the sine wave, a motion-detection cell is activated. The 2-D velocity is detected as the coordinates of this cell.

2.3.1. DS complex cells

We first state the bimodal direction tuning of model DS complex cells. Upon being stimulated with a moving spot, a group of DS complex cells is activated, and a sinusoidal firing pattern appears on the DS complex cell array (θ, τ), as shown in Fig. 5A1. Because a spot stimulus includes even components of all orientations, its firing pattern forms a complete sine wave. If a spot moves at a higher speed, the peak height increases along the τ axis, and if a spot moves at a lower speed, the peak height decreases. The phase of the sine wave shifts along the θ axis according to the direction of the spot's movement.

Suppose that target cell C_1 having the (θ_{opt}, V_{opt}) optimal velocity for a bar is stimulated by a moving spot with various velocities (Fig. 5A2). This cell is activated maximally with a moving spot having a 2-D velocity (θ_{opt}, V_{opt}), because the peak of the sinusoidal firing pattern reaches cell C_1, and thus shows a single-peak profile in the direction tuning at this speed. When a spot is moving at a higher speed, V_s; ($V_s > V_{opt}$), this cell is activated by the velocities of a set of (θ_s^-, V_s) and (θ_s^+, V_s), at which velocity the sinusoidal firing pattern passes through the point C_1. This means that the direction tuning curve at a fixed speed V_s, higher than the optimal speed, follows a bimodal profile. The directions that provide maximum response to the cell at V_s are a pair of θ_s^- and θ_s^+. Therefore, the two peaks are symmetric for the optimal direction θ_{opt}, and the interval between them, $\Delta\theta_{CC}$, splits as the speed increases. The interval is obtained by $\Delta\theta_{CC} = 2\cos^{-1}(V_{opt}/V_s)$ and expands to nearly 180° as the speed of the spot increases.

Skottun, Zhang and Grosof (1994) derived a similar relationship from the spatio-temporal filtering approach for a random-dots pattern, though they did not discuss the other type of bimodality at all.

2.3.2. Motion-detection cells

We next state the bimodal direction tuning of model motion-detection cells. Upon being stimulated with a moving bar, a group of motion-detection cells is activated, and the linear firing pattern appears on the motion-detection cell array (τ_x, τ_y), as shown in Fig. 5B1. If a bar moves at a higher speed, the linear pattern shifts away from the origin perpendicular to the pattern, and if a bar moves at a lower speed, the line shifts toward the origin. The linear pattern rotates centered around the origin according to the direction of the bar movement.

Suppose that target cell C_2 having the (θ_{opt}, V_{opt}) optimal velocity for a spot is stimulated by a moving bar with various velocities (Fig. 5B2). This cell is activated maximally with a moving bar having a 1-D velocity (θ_{opt}, V_{opt}), because the foot to the linear pattern reaches cell C_2, and thus shows a single-peak profile in the direction tuning at this speed. When a bar moving at a lower speed, V_b; ($V_b < V_{opt}$), this cell is activated by the velocities of a set of (θ_b^-, V_b) and (θ_b^+, V_b), at which velocity the linear firing pattern reaches C_2. This means that the direction tuning curve at a fixed speed of V_b, lower than the optimal speed, indicates a bimodal profile. The directions that provide maximum response to the cell at V_b are a pair of θ_b^- and θ_b^+. Therefore, the two peaks are symmetric for the optimal direction θ_{opt}, and the interval between them,

$\Delta\theta_{MDC}$, splits as the speed decreases. The interval is obtained by $\Delta\theta_{MDC} = 2\cos^{-1}(V_b/V_{opt})$ and it expands up to 180° as the speed of the bar decreases. By considering the low-speed limit, i.e. a stationary bar, it can be predicted that the optimal direction differs from the spot's optimal direction by 90°. This unusual property was previously reported as a Type-II MT neuron (Albright, 1984; Rodman & Albright, 1987, 1989).

Albright (1984) also showed a similar relationship and predicted that bimodal tuning will be observed at a low-speed bar in Type-II neurons. In a recent paper, Simoncelli and Heeger (1998) referred to a prediction of both types of bimodal tuning based on a computational model, but they described neither the mathematical relationship nor the neuronal mechanism for the bimodalities.

In summary, the model predicts that stimulus conditions for the bimodal tuning curve are as follows: (1) a spot moving at a higher than optimal speed in the model DS complex cells (i.e. component cells); and (2) a bar moving at a lower than optimal speed in the model motion-detection cells (i.e. pattern cells).

Fig. 6 shows two types of bimodal tunings that were simulated using a partially modified model we obtained in consideration of the broad tuning to speed in actual neurons (see Appendix A).

3. Experiment

3.1. Preparation

Three Japanese monkeys (*Macaca fuscata*) weighing about 6–7.5 kg were repeatedly used for our experiments. All procedures in the experiments adhered to the NIH Guide for the Care and Use of Laboratory Animals. The general methods of preparation and recording were similar to those described previously (Tanaka, Hikosaka, Saito, Yukie, Fukada & Iwai, 1986; Saito, Yukie, Tanaka, Hikosaka, Fukada & Iwai, 1986; Tanaka & Saito, 1989; Tanaka, Sugita, Moriya & Saito, 1993).

Each recording session began by applying anesthesia with 10 mg/kg of ketamine hydrochloride (in muscle). Throughout the recording, the animal was immobilized with muscle relaxant (pancuronium bromide, initially 4 μg/kg, followed by 2 μg/kg/h i.m.), and anesthesia was maintained by artificial ventilation with a 70:30 N_2O–O_2 gas mixture with 0.2% of sevoflurane.

3.2. Visual stimulation

Once a single neuron was isolated, several observations were made before quantitative testing began.

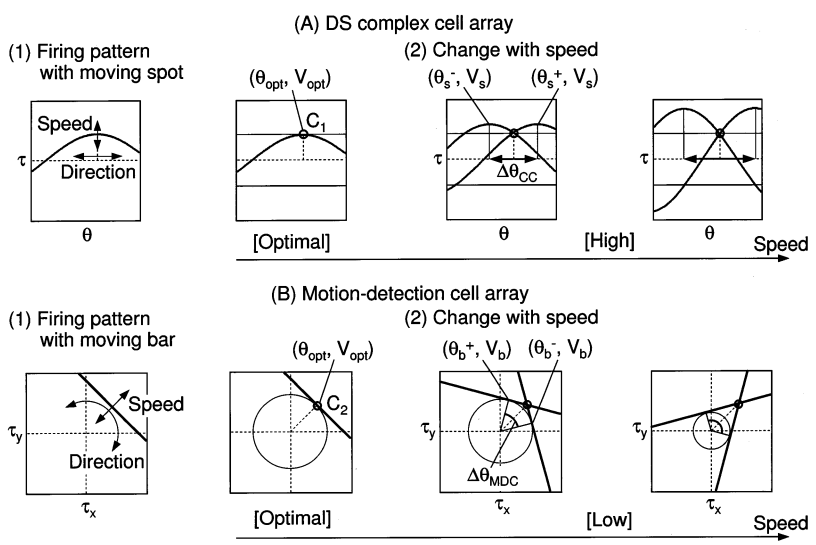

Fig. 5. The effects of changing speed and direction for the modeled cell response. (A1) When stimulated with a moving spot, a sinusoidal firing pattern appears on the DS complex cell array. According to the direction and speed of the spot, the phase and amplitude of the sine wave shift, respectively. (A2) Cell C_1, having the (θ_{opt}, V_{opt}) optimal velocity for a bar, can be activated by a spot moving at velocities of a pair of (θ_s^-, V_s) and (θ_s^+, V_s) for $V_s > V_{opt}$. Therefore, the direction tuning curve at a speed of V_s follows a bimodal profile. The interval $\Delta\theta_{CC}$ between the two peaks θ_s^- and θ_s^+ widens as the speed increases. (B1) When stimulated with a moving bar, a linear firing pattern appears on the motion-detection cell array. According to the direction and speed of the bar, the pattern rotates centered around the origin and the distance from the origin shifts. (B2) Cell C_2, having the (θ_{opt}, V_{opt}) optimal velocity for a spot, can be activated by a bar moving at velocities of a pair of (θ_b^-, V_b) and (θ_b^+, V_b) for $V_b < V_{opt}$. Therefore, the direction tuning curve at a speed of V_b follows a bimodal profile. The interval $\Delta\theta_{MDC}$ between the two peaks θ_b^- and θ_b^+ widens as the speed decreases.

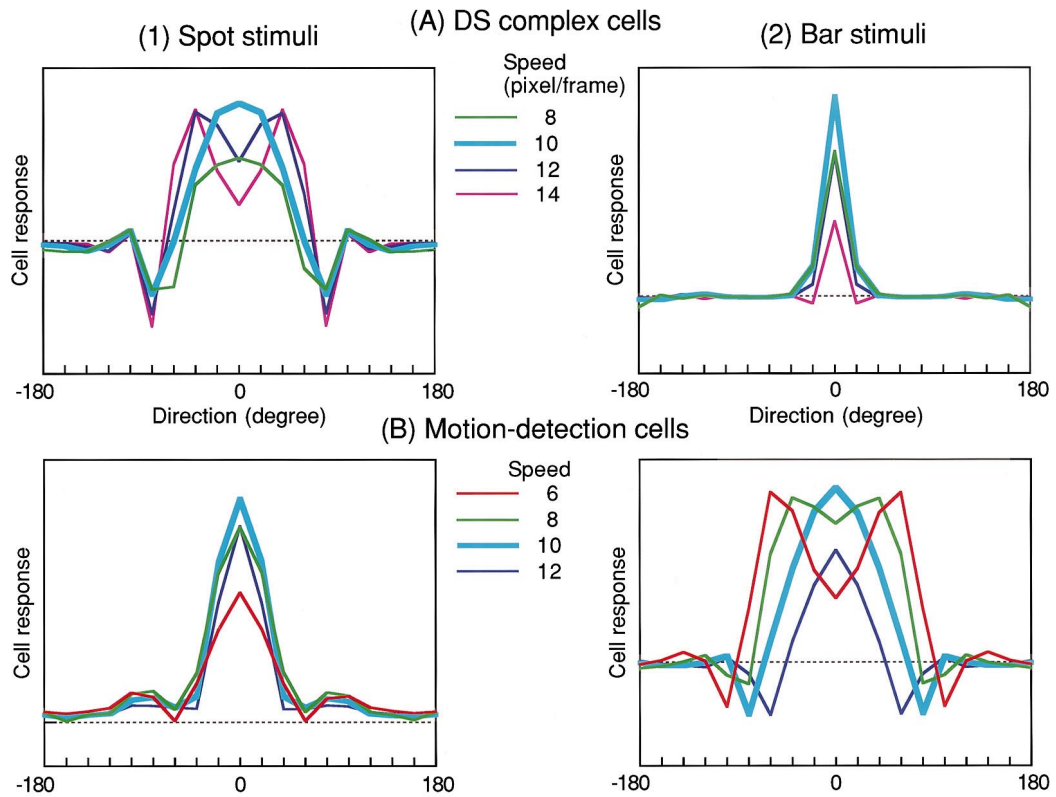

Fig. 6. Direction tuning curves of modeled DS complex (A) and motion-detection cells (B) for moving spots and bars of differing speeds. Using the model equations (Kawakami & Okamoto, 1996), we calculated the direction tuning of cells for these stimuli. The optimal speeds of both the DS complex and motion-detection cells were set to 10 pixels/frame. We depicted the tuning curves with the abscissa showing the direction of stimulus movement and the ordinate showing the cell response. The dashed line indicates the level of spontaneous activity. (A) The curves are constantly unimodal for moving bars of all speeds. In contrast, a bimodal curve appears for moving spots at speeds higher than the optimal speed. The distance between the two peaks widens as the spot speed increases. (B) The curves are constantly unimodal for moving spots of all speeds. A bimodal curve appears for moving bars at speeds lower than the optimal speed. The distance between the two peaks widens as the bar speed decreases.

These observations were made using real hand-held objects and computer drawings moved by a mouse. The optimal values of stimulus parameters such as direction, speed, and size were estimated using the eye contralateral to the recording site. The profile of its receptive field was then estimated using the optimal stimulus.

Quantitative testing was performed using visual stimuli on the CRT display, placed at 50 cm from the cornea and subtending about $15 \times 15°$ of the visual field. The movement of such stimuli was accurately controlled by a personal computer (with a refresh rate of 56 Hz). The distance to the display was sometimes decreased to cover the whole receptive field of the recording neuron. We used a bright contrast for the moving stimulus on a dark background because the response properties in MT neurons are invariant in contrast polarity. Two types of stimuli were used for comparison: (1) moving spots, these stimuli were single solid circles of the smallest size possible that gave a reliable response, the spot diameter generally ranged from 0.16 to 0.8°; (2) moving bars: these stimuli extended slightly beyond the borders of the receptive field, except when a remarkable surrounding inhibition was observed. The bar length ranged from 4 to 16°, and the bar width ranged from 0.1 to 0.4°. In most cases, the diameter of the moving spot was twice the width of the bar at each neuron. The direction of the moving bar was orthogonal to its orientation. In the latter part of this paper, the terms 'spot' and 'bar' also mean 'moving spot' and 'moving bar', respectively.

Each moving stimulus at a given speed was presented in 18 directions of motion with a constant angular deviation (20°). The same 18 directions were used for all tests on each neuron, and opposite directions were paired and presented in sequential order. Each test consisted of 10 repetitions of the presentation of 18 directions. The CRT display was centered on the neuron's receptive field, and the moving stimuli were controlled so as to pass across the center of the receptive field in all directions. The excursion of moving stimuli was set to sweep beyond the receptive field, ranging from 8 to 16°. One second after the start of measurement in each direction, the visual stimulus appeared at the start position on the display and began to move.

After the moving stimulus disappeared, measurements continued for about another second. Thus, the interval of each presentation was normally about 2 s. The direction is defined such that the movement to the right was 0° and increased one revolution in a counterclockwise direction. In some figures, for example, we used −180° for a direction of 180°.

In the beginning of the quantitative test, we classified cell types as component-motion selective or pattern-motion selective using another kind of stimulus, which is called a 'moving cross'. This stimulus is a composite of two bars moving independently in orthogonal directions. Except for the direction of motion, all parameters of both bars were identical. This stimulus may be observed as a moving cross through a local window, such as a receptive field. We supposed that the relationship of a moving bar to a moving cross is equivalent to the relationship of a moving grating to a moving plaid. Moreover, we think that the moving cross is more essential than a moving plaid in the sense that it does not contain many cross-points (as contained in the plaid), which themselves could be a strong stimulus feature for the motion-detection pathway. From these considerations, we used the moving cross to distinguish the type of recording neurons in this study. We defined the direction of the moving cross as the direction of movement of the intersection point of the two component bars. The directions of each moving bar, therefore, are 45° different than the direction of the moving cross. The speed of the moving cross is also defined by the speed of its component bars. A moving cross was also presented in 18 directions, as was a spot and a bar, at approximately the optimal speed. We determined cell type by whether it responded to the movement of the component bar or the whole cross.

3.3. Recording

Extracellular single-cell recordings were made in the deep portion of the superior temporal sulcus using a glass-coated platinum-iridium microelectrode (2–3 MΩ at 1 kHz). The electrode was advanced in the horizontal plane anteromedially at an angle of 40° to the parasagittal plane. Because the electrode detects a signal only from cell bodies and detects no signal from fibers, the region between gray matter and white matter can be differentiated and, thus, the boundary of the cortex can be determined.

Most of the recordings were made from the cortex in MT representing the central 20° of visual field. Background activity was amplified and displayed on an oscilloscope. Spikes were judged to arise from an isolated single neuron if they appeared constant in amplitude and waveform. The activity of a single isolated neuron was converted into digital pulses. The generated time of the digital pulses was collected and displayed on-line as peristimulus time histograms (PSTH) to enable analysis of the firing rate during stimulus presentation.

3.4. Procedure for individual neurons

The experiment commenced following preparation of the animal and insertion of the microelectrode into the target position. We first used a moving cross to classify the type of target neurons as either component, pattern, or unclassified. If the direction tuning curve estimated from the on-line PSTH showed a bimodal profile, we classified it as a component type, and if the curve showed a unimodal profile, we judged it to be a pattern type. In the case where classification was difficult, we determined it to be unclassified. We skipped the following test on neurons having no clear tuning profile. We then proceeded with the main measurement using moving spots and bars to validate the bimodal direction tuning curve under predicted conditions. We started with measurements from the optimal speed previously estimated and continued recordings at different speeds of motion, giving priority to the range of speed in which bimodality was expected. The speed was varied at several levels in the range of 2–5 octaves for both the spots and the bars. After obtaining a complete set of moving spot and bar speeds, which took at least 3 h, we proceeded to the next neuron.

3.5. Data analysis

We constructed the direction tuning curves for each speed for both the spots and bars. We used the mean firing rate, i.e. an averaged spike number in a time window, as the neuronal activity. The width of the time window was selected to correspond roughly to the whole range of the receptive field and was fixed at the same speed for three types of moving stimuli. The spontaneous firing rate was also calculated from the beginning of 1 s of PSTHs and was averaged over all 18 directions. The value of the mean firing-rate, subtracting the average spontaneous firing-rate from the raw mean firing-rate, was used to construct the direction tuning curves and evaluate the response properties in additional analyses. Taking into account the total profiles of the direction tuning curves for both the spots and bars at a variety of speeds, we compared the response properties of recorded neurons with the model prediction, focusing on the appearance of bimodality. The distribution of the optimal speed, the index of directionality (DI), and the direction tuning-width were also studied (see the section on results) using this data.

4. Results

4.1. Classification of MT neurons

Quantitative testing using computer controlled stimuli was carried out for a total of 56 MT neurons recorded along 24 penetrations in the three monkeys. The results are summarized in Table 1. Typical tuning curves for a moving cross are shown in Fig. 7. When the tuning curve had two clear peaks separated by 90°, we classified the neuron as 'component type' (21 neurons). In contrast, when the curve had a single main peak, it was classified as 'pattern type' (18 neurons). Neurons that were clearly directionally-selective but difficult to distinguish between bimodal and unimodal from their tuning profile were classified as 'unclassified type' (14 neurons). Many of the unclassified cells showed two peaks in direction tuning, but the heights of the peaks were asymmetric. The three neurons that revealed no clear directional selectivity were excluded from this classification. We validated the model based on 35 neurons, by measuring at various speeds with the moving spot and moving bar, of these 56 neurons.

The distribution of the recording site of most of these neurons is depicted for each cell type in Fig. 8. The origin of the abscissa indicates a boundary between layer 6 of area MT and the cortical white matter, and the value of the abscissa gradually increases toward the cortical surface along the penetration track. It is therefore not necessarily equal to the depth because the penetrations could be oblique to the cortical surface. These graphs demonstrate the difference in distribution between the component type and the pattern type neurons; the former were distributed mainly in the deeper half of the cortex, while the latter were located mainly in the shallower half. This observation provides clear evidence for the existence of a layer structure of two types of neurons in area MT.

Table 1
Total MT neurons

	Number of neurons (type: C/P/U/N)[a]
Total neurons	56 (21/18/14/3)
Excluded from validation	21 (6/4/8/3)
Used for validation	35 (15/14/6/0)
Bimodal	10 (6/4/0/0)
Constantly unimodal	13 (3/7/3/0)
Contradictory bimodal	1 (0/1/0/0)
Directionally unstable	11 (6/2/3/0)

[a] C, component type; P, pattern type; U, unclassified type; N, not determined.

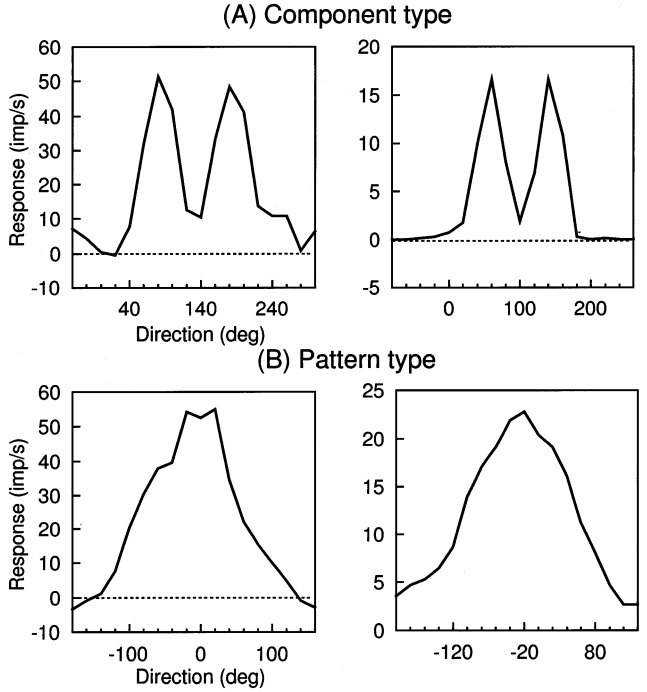

Fig. 7. Direction tuning curves for four representative MT neurons recorded with a moving cross. The response intensity, the mean firing rate from which the spontaneous spike rate was subtracted, was plotted against the direction of stimulus movement. (A) Typical component type having two split peaks separated by 90°. These two peaks indicate the selective responses to the motion of the component bars of cross stimulus. The preferred direction of this neuron was estimated to be the direction of the trough between the two peaks. (B) Typical pattern type having a single main peak. The direction of the peak, i.e. the preferred direction of this neuron, was consistent with the direction of motion of the intersection made up by two component bars. The abscissa indicates the direction of motion and the ordinate indicates cell activity defined by the mean firing rate. The dashed line indicates the level of spontaneous activity, defined as zero.

4.2. Validating the two types of predicted bimodality

Fig. 9 illustrates the bimodal tuning curve recorded from four representative MT neurons. This presents the direction tuning curves at all speeds measured with the moving spot and moving bar. Three neurons in Fig. 9(A–C) were judged to be model DS complex cells, while one neuron in Fig. 9(D) was judged to be a model motion-detection cell. The pictures in the left column in each row indicate the tuning curves for the moving cross. In Fig. 9(A–C), because the tuning curves had two clear peaks separated by 90°, they were classified as component type. In contrast, Fig. 9(D) was classified as pattern type because of its single main peak in the curve.

The tuning curves for the moving spot are depicted in the center column in Fig. 9, and those for the moving bar are depicted in the right column. In Fig. 9(A–C), the tuning curves for the bar are unimodal and almost

constant, as in Fig. 6A2. Their optimal directions match the direction of the trough of the two peaks of the curves for the cross. On the other hand, the curves for the moving spot were unimodal at a low speed but gradually widened as the speed increased. At the highest speed, the curve showed a clear bimodal shape. These bimodal tuning curves are consistent with the predicted curves in Fig. 6A1. The neuron in Fig. 9(D), in contrast, showed constant unimodal tuning curves for the moving spot, as in Fig. 6B1. The optimal direction matches that of the tuning curves for the moving cross. The tuning curve for the moving bar was also unimodal at high speeds, though it changed to bimodal at the lowest speed. These tuning curves are consistent with the predicted curves in Fig. 6B2. The neurons in Fig. 9(B) and (D) were recorded on the same penetration track but at different depths.

Other neurons are shown in Fig. 10: the neuron on the top was determined to be a DS complex cell, and the two neurons at the bottom were determined to be motion-detection cells. These neurons also revealed responses similar to those predicted by the model, but not as clearly as the neurons in Fig. 9. The representative speeds that revealed both unimodal and bimodal tuning curves were selected, and the intensity of each response was normalized to clarify the differences in the tuning profile. The bimodal curve of the DS complex cells (Fig. 10A1) was asymmetric, and the troughs of the motion-detection cell curves (Fig. 10B2, C2) were not

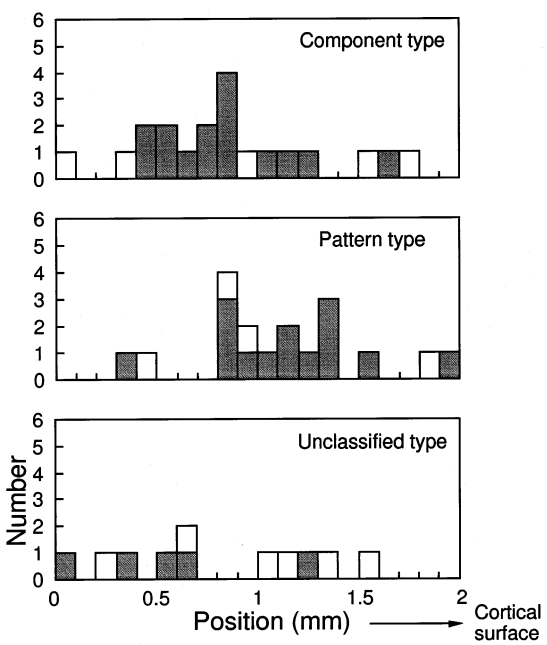

Fig. 8. Recording site of MT neurons. Top, component type; center, pattern type; bottom, unclassified type. The shadowed histogram indicates the cells included in 35 neurons used for validation of the model. The abscissa indicates the distance from the bottom of the cortex along the penetration track.

significantly different, though they did show a tendency to change from unimodal to bimodal.

4.3. Additional measures of speed tuning

We performed additional analysis of recorded data and investigated the general properties of MT neurons by comparing cell types by component–pattern classification. In addition to the 35 neurons described above, we included three more on which directional selectivities for both spots and bars for at least one speed were tested.

4.3.1. Optimal direction

The optimal direction of 38 MT neurons was analyzed, and a comparison was made between the moving spot and the moving bar. The optimal direction was determined for moving spots and bars independently, taking into account the most intensive response within all of the speeds tested. Therefore, the selected speeds, defined to be the optimal speeds, for spots and bars were not necessarily identical in each neuron.

A significant correlation between moving spots and bars was observed in Fig. 11. Optimal directions were more or less different in many neurons, though none of the neurons showed a difference of more than 90°. Although this difference is supposedly attributable to cell response fluctuations, especially at high speed, this variance is probably also attributable to an alteration in the optimal direction according to speed, as predicted by the model. We did not observe a significant relationship between component, pattern, or unclassified cell types. These results are in agreement with our prediction.

We also calculated the index of directionality (DI) of these neurons in the optimal direction at the optimal speed. The DI was computed by

$$\mathrm{DI} = 1 - (\text{opposite response/preferred response})$$

The results were as follows: spot for component type, median = 0.95; bar for component, median = 1.00; spot for pattern type, median = 1.01; bar for pattern, median = 1.02. The distribution of DI (not shown here) centered around the value of 1.0; each histogram of moving spots and bars was similar to the previous study (Albright, 1984), though some differences appeared after taking cell type into consideration. The most notable feature was that the distribution for the moving spot of the component type had a wider expanding range than the pattern type, which probably reflects the bimodal tendency of spots in component cells.

4.3.2. Tuning bandwidth

We also calculated the tuning bandwidth; the full width of the tuning curve at one-half of its maximum

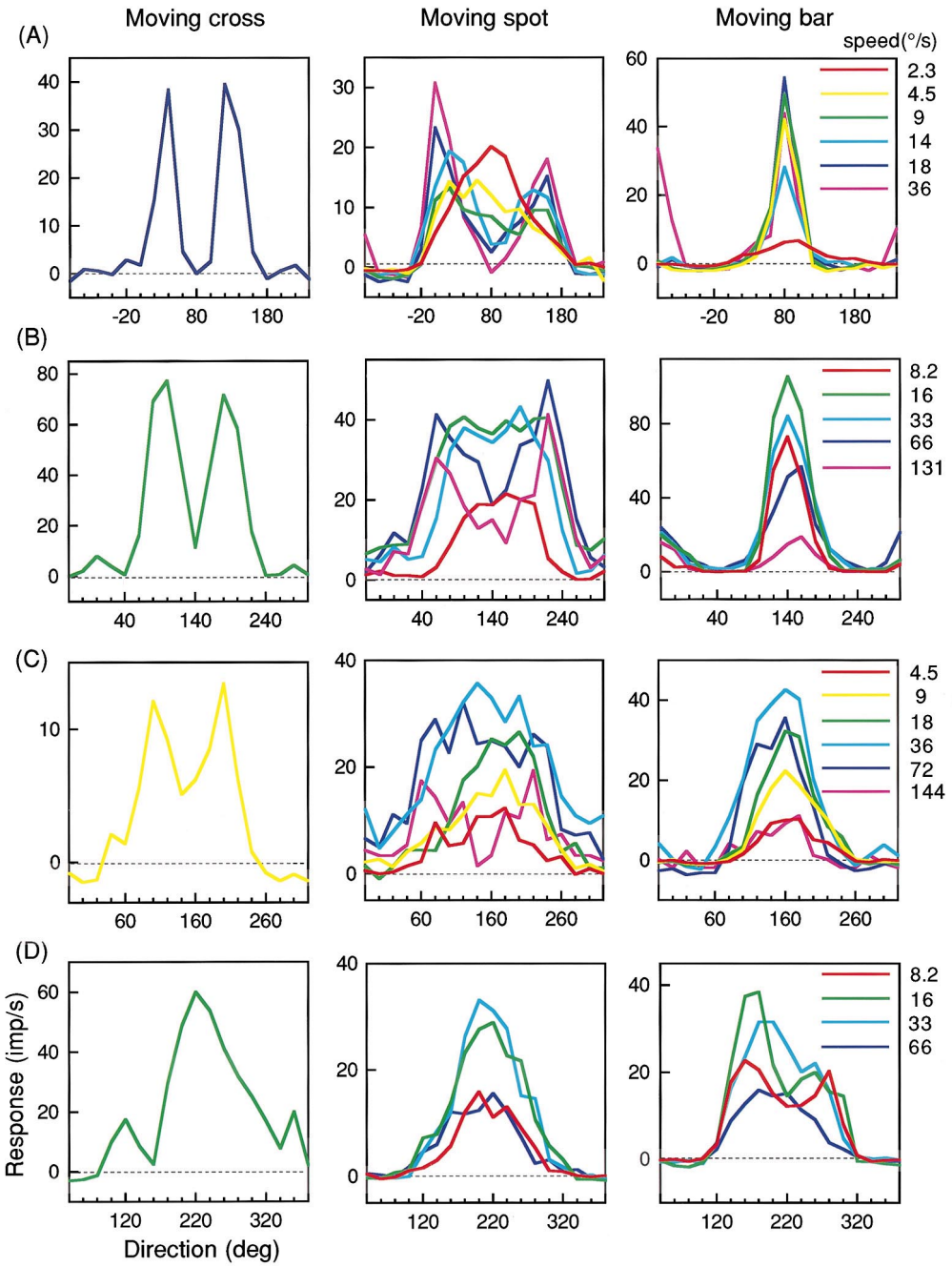

Fig. 9. Bimodal direction tuning curves of four representative neurons. The three neurons on the top (A–C) were judged to be model DS complex cells and the neuron at the bottom (D) was judged to be a model motion-detection cell. Left, tuning curves for moving cross; center, tuning curves for moving spot; right, tuning curves for moving bar.

height (Fig. 12). The speed used here was also the same as that for the optimal direction and the index of directionality on each neuron. The averaged bandwidth for spots and bars was 113 and 94°, respectively, which is similar to previous data (Maunsell & Van Essen, 1983; Albright, 1984). However, upon comparing component type and pattern type neurons, a remarkable difference was observed. The scattered plots were separated according to the dashed line, which means that the tuning bandwidth for moving spots of a component type is generally larger than that for moving bars, and is the opposite in the case of a pattern type. This tendency is consistent with that predicted by the model.

5. Discussion

5.1. Bimodality in other studies

Bimodal direction-tuning curves for a moving stimulus have been observed in earlier studies. Hammond and colleagues reported that bimodal direction tuning for a texture motion (drifting random dots) was recorded in some complex cells of the striate cortex of cats (Hammond, 1978; Hammond & Reck, 1980; Hammond & Smith, 1983). They reported that the tuning curve for moving bars was always unimodal, though the curve for random-dot patterns alternated between unimodal and bimodal as the speed increased. Later studies reported similar bimodality in simple and complex cells of the striate cortex of cats using random-dot movement (Skottun, Grosof & De Valois, 1988; Skottun et al., 1994). The random-dot pattern is equivalent to a single spot in that it almost uniformly includes all orientational components. Moreover, most of the directionally selective cells in the cat striate cortex are reported to be component-motion selective (Movshon et al., 1985). Therefore, all of this data can be explained by the predicted responses for our model DS complex cells.

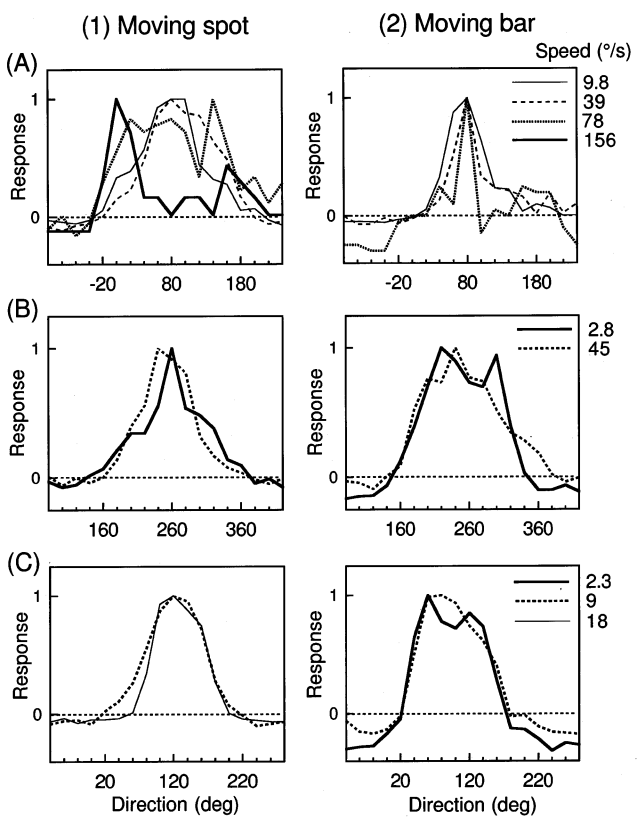

Fig. 10. Examples of cells that could not be examined for full stimulus conditions but indicated a bimodal tendency in direction tuning under predicted conditions. The curves at some speeds were selected, and the responses were normalized to facilitate the comparison. (A), DS complex cells, (B),(C), motion-detection cells. Left, tuning curves for moving spot; right, for moving bar.

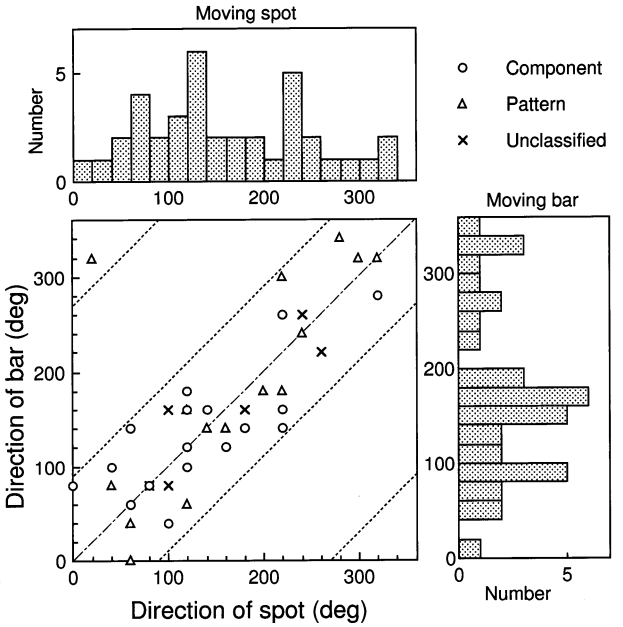

Fig. 11. Relationships between the optimal direction for the spot and that for the bar plotted against 38 MT neurons (Scatter diagram). The top histogram shows the distribution of the optimal direction for the moving spot and the right histogram shows that for the moving bar. In the scatter diagram, the component type cell was plotted with open circles, the pattern type with open triangles, and the unclassified type with crosses. The dashed line indicates the divergence of spot and bar from 90°.

As for bimodal direction-tuning for a moving bar, Albright (1984) reported the existence of such cells in monkey MT. To our knowledge, this is the only previous report of such cells. Albright also proposed a model and predicted that the bimodality for bars will occur at low speeds. However, Rodman and Albright (1987) failed to record the predicted bimodality in the subsequent experiment. Simoncelli, Bair, Cavanaugh and Movshon (1996) reported that bimodal tuning for low-speed sinusoidal gratings was obtained from some MT pattern cells, but Simoncelli and Heeger (1998) pointed out that this was due to the fact that gratings were used instead of bars. Thus, our study is the first systematic study of bimodal direction tuning for a bar in area MT of the monkey.

5.2. Considerations on the results

In this study, the bimodal direction tuning as predicted by the model was recorded in ten neurons. We determined this recording data to be clear responses of the model prediction based on the following criteria: (1) a bimodal curve appears for either a high-speed moving spot for a DS complex cell, or a low-speed moving bar for a motion-detection cell, as predicted; (2) component type and pattern type neurons classified for the moving

cross are consistent with the DS complex cell and motion-detection cell of the model, respectively; (3) the direction of the peak of unimodal tuning curves is always identical to the direction of the trough of bimodal tuning curves, the directions of two peaks must be symmetric in the optimal direction; and (4) the change of the tuning curves from unimodal to bimodal with speed is observed.

However, we failed to observe a clear bimodal tuning in other neurons (25/35). The reasons for this observation are considered below.

It is probable that for some MT neurons the range of speeds measured was not sufficiently wide to observe bimodality. We measured direction tunings at speeds up to five octaves. Nevertheless, neurons having considerably broad tuning for a speed will show a similar directional selectivity at various speeds. In this respect, it is possible that some of the 13 neurons that showed constant unimodal direction tuning (see Table 1) would change the tuning profile to bimodal if the speed of the stimulus was changed further from the optimal.

In addition, the bimodal tuning curve was hard to record from MT neurons in a sufficient signal-to-noise ratio because the peak of response magnitude decreased as the speed shifted from the optimal. This reduction in MT neuron response was more significant than expected from the calculation in the model neuron.

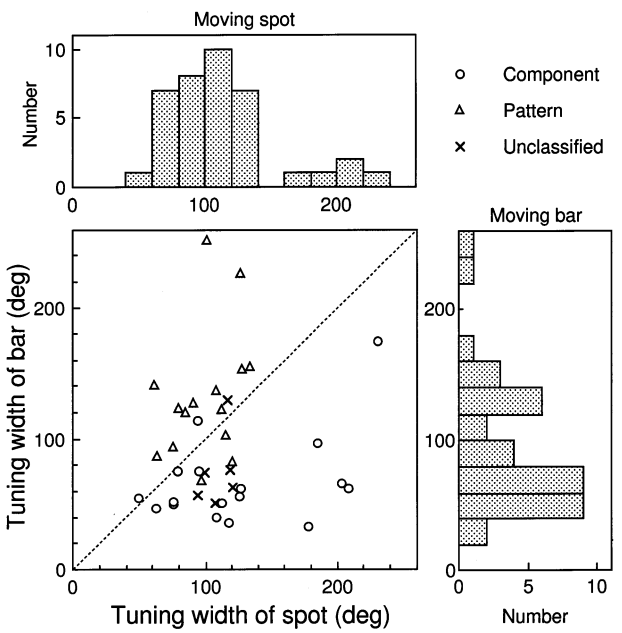

Fig. 12. Tuning bandwidth for the same 38 MT neurons as in Fig. 11. See also the legend to Fig. 11. We observed a remarkable distribution difference between component and pattern types in the scatter diagram. The mean bandwidth of component cells for the spot stimulus is 125° and for the bar stimulus is 67°. The mean bandwidth of pattern cells for the spot stimulus is 100° and for the bar stimulus is 133°.

Finally, we believe the contamination of cell responses by various visual factors such as surround motion (Tanaka et al., 1986) and transient on/off signals make it difficult to observe bimodal direction tunings. It should be noted that, though we were careful to eliminate such effects, it is still possible that responses were contaminated.

5.3. New idea for velocity selectivity

In previous studies by various researchers, response properties of MT neurons were usually analyzed using a method that involved estimating the direction tuning at an optimal speed and the speed tuning in an optimal direction. The peak on those tuning curves was regarded as indicating the optimal velocity (direction and speed) of the neuron concerned. Thus, MT neurons were considered to have a unique and particular velocity at which they respond selectively to visual stimuli, i.e. the optimal velocity. However, our model proposes a new idea regarding velocity representation in area MT and an extended concept of velocity selectivity in MT neurons.

We first discuss velocity representation in area MT. Two kinds of the firing patterns derived from the model are shown in Fig. 5: a sinusoidal firing pattern on the array of DS complex cells by stimulation with a moving spot (Fig. 5A1); and a linear firing pattern on the array of motion-detection cells by stimulation with a moving bar (Fig. 5B1). These firing patterns indicate that the velocity is not represented in MT in a fixed manner by fixed preferred neurons, but is represented by different groups of neurons for different stimuli. The distribution of neurons that represent velocity information changes significantly according to moving stimulus differences, i.e. a spot or a bar. The distribution pattern of active neurons differs according to cell-type (i.e. component or pattern type) by which the cell array is constructed. In specific cases, such as DS complex cells for a moving bar or motion-detection cells for a moving spot, the velocity is represented by a single neuron tuned to the velocity considered thus far.

We then discuss velocity selectivity of MT neurons. In Section 2.3, we showed that some velocity sets of a moving spot, (θ_s, V_s), maximize activation of a model DS complex cell. In detail, the distribution map of these (θ_s, V_s) forms a line on the (V_x, V_y) velocity space, and the bimodal direction tuning is obtained by intersecting the line at a fixed speed (Kawakami & Okamoto, 1996), which means that a DS complex cell does not have a unique optimal velocity but has various preferred velocities for a moving spot. In the same way, we can say that a motion-detection cell also has various preferred velocities for a moving bar. We selected a spot and a bar as a stimulus because the former is a typical spatial pattern that has even components of every orientation,

and the latter is a typical spatial pattern that has the most localized orientation component. Any visual stimulus will have an intermediate property between spots and bars. Therefore, we can say in general that velocity selectivity is determined by cell type and the spatial pattern of a visual stimulus.

Although the concept of velocity selectivity in our model is different from the conventional concept, there is no conflict. As shown in computer simulation, response decreases at speeds exhibiting a bimodal profile. Within the distribution of preferred velocities on the velocity space, the most sensitive velocity is consistent with the conventional optimal velocity and is identical for a spot and a bar. Hence, we can say that the model extends the concept of velocity selectivity and involves the conventional concept.

6. Conclusion

We measured the activities of single neurons in the visual area MT of monkeys and studied directional selectivity for various visual stimuli. Our model for local velocity detection predicted two contrasting types of bimodal direction tunings for two kinds of MT neurons: component cells; and pattern cells. The prediction of the model was summarized below. (i) DS complex cells (corresponds to component cells). The direction tuning indicated a bimodal profile for moving spots at high speed. It also showed a unimodal profile for moving spots at low speed or for moving bars at any speed. The angular separation between the two peaks increases as the spot's speed increases. (ii) Motion-detection cells (corresponds to pattern cells). The direction tuning indicated a bimodal profile for moving bars at low speed. It also revealed a unimodal profile for moving bars at high speed or for moving spots at any speed. The angular separation between the two peaks increases as the bar's speed decreases.

Out of 56 MT neurons, with a moving cross and measurements taken at various moving spot and bar speeds, we classified 15 neurons as component type, 14 as pattern type, and the remaining six as unclassified type. Within these 35 neurons, we recorded six component cells and four pattern cells showing the predicted bimodality in their direction tunings, which lends neurophysiological support to the validity of the proposed model. This is the first study that records the bimodal tuning curve of two types of MT neurons in monkeys and clarifies the neuronal mechanism of both types of bimodalities. In addition, the results imply a new concept for velocity selectivity of MT neurons, i.e. velocity selectivity is determined by the cell type (component or pattern) and the spatial pattern of the visual stimulus.

Acknowledgements

We thank Dr Seiya Ogawa and Shigeru Sato of Fujitsu Laboratories Ltd. for their encouragement during this work. This work was supported in part by a Grant-in-Aid for Scientific Research on Priority Areas # 08279102, The Ministry of Education, Science, Sports, and Culture of Japan, and by a Grant-in-Aid (JSPS-RFTF96I 00104) from the Japanese Society for the Promotion of Science Research for the Future Program to H.S.

Appendix A. Partial modification of the model

In the simulation of direction tuning curves for moving spots and moving bars (Fig. 6), we slightly modified the model previously reported (Kawakami & Okamoto, 1996). Considering the broad tuning of actual MT neurons to speed, we introduced a divergent connection between the DS simple cells and the DS complex cells, which is equivalent to the convergent connection from the former model DS complex cells to the modified model DS complex cells, as schematically illustrated in Fig. A1. Summing up the responses of the DS simple cells tuned to various speeds, the DS complex cells acquire sensitivity to a wide range of visual stimulus speeds. Thus, the DS complex cells acquire broad speed-tuning. Here we added inhibitory connections to convey inhibitory responses, modeled the lateral inhibition mechanism, and assumed that only the excitatory responses of the DS simple cells are conveyed to the DS complex cells. The other properties of the model cells,

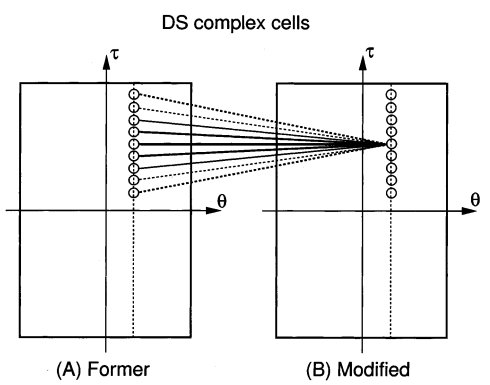

Fig. A1. Schematic illustration of partial modification of the model DS complex cells. Convergent connections from the former DS complex cells to the modified DS complex cells were introduced. In fact, these connections were projected directly from the former DS simple cells to the modified DS complex cells. The solid line indicates the excitatory connections, and the dashed line indicates the inhibitory connections. The thick line indicates a high connection weight, and the thin line indicates a low connection weight. Only the excitatory responses of former DS simple cells are assumed to be conveyed to the modified DS complex cells. Thus, the modified DS complex cells respond to a wide range of visual stimulus speeds.

however, are invariant with this modification. As for further development of our model, we are planning to propose a more sophisticated model that includes intracortical connections among columns (Okamoto & Kawakami, 1996).

References

Adelson, E. H., & Bergen, J. R. (1985). Spatiotemporal energy models for the perception of motion. *Journal of the Optical Society of America A*, *2*, 284–299.

Adelson, E. H., & Movshon, J. A. (1982). Phenomenal coherence of moving visual patterns. *Nature*, *300*, 523–525.

Albright, T. D. (1984). Direction and orientation selectivity of neurons in visual area MT of the macaque. *Journal of Neurophysiology*, *52*, 1106–1130.

Borst, A., & Egelhaaf, M. (1989). Principles of visual motion detection. *Trends in Neurosciences*, *12*, 297–306.

Duda, R. O., & Hart, P. E. (1972). Use of the Hough transformation to detect lines and curves in pictures. *Communications ACM*, *15*, 11–15.

Fennema, C. L., & Thompson, W. B. (1979). Velocity determination in scenes containing several moving objects. *Computer Vision, Graphics, and Image Processing*, *9*, 301–315.

Grzywacz, N. M., & Yuille, A. L. (1990). A model for the estimate of local image velocity by cells in the visual cortex. *Proceedings of the Royal Society of London B*, *239*, 129–161.

Hammond, P. (1978). Directional tuning of complex cells in area 17 of the feline visual cortex. *Journal of Physiology*, *285*, 479–491.

Hammond, P., & Reck, J. (1980). Influence of velocity on directional tuning of complex cells in cat striate cortex for texture motion. *Neuroscience Letters*, *19*, 309–314.

Hammond, P., & Smith, A. T. (1983). Directional tuning interactions between moving oriented and textured stimuli in complex cells of feline striate cortex. *Journal of Physiology*, *342*, 35–49.

Heeger, D. J. (1987). Model for the extraction of image flow. *Journal of the Optical Society of America A*, *4*, 1455–1471.

Hough, P. V. C. (1962). Method and means for recognizing complex patterns. *U.S. Patent* 3069654.

Humphrey, A. L., & Weller, R. E. (1988). Functionally distinct groups of X-cells in the lateral geniculate nucleus of the cat. *Journal of Comparative Neurology*, *268*, 429–447.

Kawakami, S., & Okamoto, H. (1996). A cell model for the detection of local image motion on the magnocellular pathway of the visual cortex. *Vision Research*, *36*, 117–147.

Lagae, L., Raiguel, S., & Orban, G. A. (1993). Speed and direction selectivity of macaque middle temporal neurons. *Journal of Neurophysiology*, *69*, 19–39.

Marr, D., & Ullman, S. (1981). Directional selectivity and its use in early visual processing. *Proceedings of the Royal Society of London B*, *211*, 151–180.

Mastronarde, D. N. (1987a). Two classes of single-input X-cells in cat lateral geniculate nucleus. 1. Receptive-field properties and classification of cells. *Journal of Neurophysiology*, *57*, 357–380.

Mastronarde, D. N. (1987b). Two classes of single-input X-cells in cat lateral geniculate nucleus. 2. Retinal inputs and the generation of receptive-field properties. *Journal of Neurophysiology*, *57*, 381–413.

Maunsell, J. H. R., & Van Essen, D. C. (1983). Functional properties of neurons in middle temporal visual area of the macaque monkey. 1. Selectivity for stimulus direction, speed, and orientation. *Journal of Neurophysiology*, *49*, 1127–1147.

Maunsell, J. H. R., & Newsome, W. T. (1987). Visual processing in monkey extrastriate cortex. *Annual Review of Neuroscience*, *10*, 363–401.

Mikami, A., Newsome, W. T., & Wurtz, R. H. (1986a). Motion selectivity in macaque visual cortex. 1. Mechanisms of direction and speed selectivity in extrastriate area MT. *Journal of Neurophysiology*, *55*, 1308–1327.

Mikami, A., Newsome, W. T., & Wurtz, R. H. (1986b). Motion selectivity in macaque visual cortex. 2. Spatiotemporal range of directional interactions in MT and V1. *Journal of Neurophysiology*, *55*, 1328–1339.

Movshon, J. A., Adelson, E. H., Gizzi, M. S., & Newsome, W. T. (1985). The analysis of moving visual patterns. In C. Chagas, R. Gattass, & C. Gross, *Experimental brain research supplementum II: pattern recognition mechanisms* (pp. 117–151). New York: Springer.

Ogata, M., & Sato, T. (1991). Motion perception model with interaction between spatial frequency channels. *Systems and Computers in Japan*, *22*, 30–39.

Okamoto, H., & Kawakami, S. (1996). A basic model for the intercolumnar connections on the local motion detection. In *1996 Annual Conference of Japanese Neural Network Society* (pp. 225–226) (in Japanese).

Reichardt, W. (1961). Autocorrelation, a principle for evaluation of sensory information by the central nervous system. In W. A. Rosenblith, *Principles of sensory communication* (pp. 303–317). New York: Wiley.

Rodman, H. R., & Albright, T. D. (1987). Coding of visual stimulus velocity in area MT of the macaque. *Vision Research*, *27*, 2035–2048.

Rodman, H. R., & Albright, T. D. (1989). Single-unit analysis of pattern-motion selective properties in the middle temporal visual area (MT). *Experimental Brain Research*, *75*, 53–64.

Saito, H-A., Yukie, M., Tanaka, K., Hikosaka, K., Fukada, Y., & Iwai, E. (1986). Integration of direction signals of image motion in the superior temporal sulcus of the macaque monkey. *Journal of Neuroscience*, *6*, 145–157.

Saul, A. B., & Humphrey, A. L. (1990). Spatial and temporal response properties of lagged and nonlagged cells in cat lateral geniculate nucleus. *Journal of Neurophysiology*, *64*(1), 206–224.

Sereno, M. E. (1993). *Neural computation of pattern motion*. Cambridge, MA: MIT Press.

Simoncelli, E. P., Bair, W. D., Cavanaugh, J. R., & Movshon, J. A. (1996). Testing and refining a computational model of neural responses in area MT. *Investigative Ophthalmology and Visual Science Supplement*, *37*, 916.

Simoncelli, E. P., & Heeger, D. J. (1998). A model of neuronal responses in visual area MT. *Vision Research*, *38*, 743–761.

Skottun, B. C., Grosof, D. H., & De Valois, R. L. (1988). Responses of simple and complex cells to random dot patterns: a quantitative comparison. *Journal of Neurophysiology*, *59*, 1719–1735.

Skottun, B. C., Zhang, J., & Grosof, D. H. (1994). On the directional selectivity of cells in the visual cortex to drifting dot patterns. *Visual Neuroscience*, *11*, 885–897.

Tanaka, K., Hikosaka, K., Saito, H-A., Yukie, M., Fukada, Y., & Iwai, E. (1986). Analysis of local and wide-field movements in the superior temporal visual areas of the macaque monkey. *Journal of Neuroscience*, *6*, 134–144.

Tanaka, K., & Saito, H-A. (1989). Analysis of motion of the visual field by direction, expansion/ contraction, and rotation cells clustered in the dorsal part of the medial superior temporal area of the macaque monkey. *Journal of Neurophysiology*, *62*, 626–641.

Tanaka, K., Sugita, Y., Moriya, M., & Saito, H-A. (1993). Analysis of object motion in the ventral part of the medial superior

temporal area of the macaque visual cortex. *Journal of Neurophysiology*, *69*, 128–142.

Van Santen, J. P. H., & Sperling, G. (1985). Elaborated Reichardt detectors. *Journal of the Optical Society of America A*, *2*, 300–321.

Watson, A. B., & Ahumada Jr, A. J. (1985). Model of human visual-motion sensing. *Journal of the Optical Society of America A*, *2*, 322–341.

Zeki, S. M. (1974). Functional organization of a visual area in the posterior bank of the superior temporal sulcus of the rhesus monkey. *Journal of Physiology*, *236*, 549–573.